JOURNAL OF NATURAL REMEDIES
DOI: 10.18311/jnr/2025/49647

RESEARCH ARTICLE

Computational Studies and Chromatographic Profiling of Aristolochic Acid from Roots of *Aristolochia indica* L. as a PLA2 Inhibitor against the Four Poisonous Indian Snake Venoms

R. S. David Paul Raj[1*], W. Andrea Bernice[1], M. Beutline Malgija[2], S. Kavinila[1], J. Jannet Vennila[2], B. Jebasingh[3] and D. Premnath[1]

[1]Division of Biotechnology, School of Engineering and Technology, Karunya Institute of Technology and Sciences, Coimbatore - 641114, Tamil Nadu, India; dpaulraj1976@gmail.com

[2]Centre for Computational Informatics, MCC-MRF Innovation Park, Madras Christian College, Chennai - 600059, Tamil Nadu, India

[3]Division of Applied Chemistry, School of Sciences, Arts and Media, Karunya Institute of Technology and Sciences, Coimbatore - 641114, Tamil Nadu, India

Abstract

Background: Envenomation caused by snakebite is a rapidly developing, extremely dangerous condition that is unlike any other acute illness, contributing to an alarming global mortality of 81,000 deaths annually, according to World Health Organization (WHO) reports. The common venomous snakes found in India are Cobra (*Naja naja*), Krait (*Bungarus caeruleus*), Russell's viper *(Daboia russelli*), and Saw Scaled viper (*Echis carinatus*). Snake venoms contain many toxins endowed with phospholipase A2 (PLA2) activity. Treatments for snake bites include a vast collection of medicinal plants. **Aim:** Traditional healers employ the medicinal herb *Aristolochia indica* L., belonging to the family *Aristolochiaceae*, as a good source of anti-venom. Despite its known bioactive chemicals, the specific metabolites responsible for inhibiting PLA2 in snake venoms remain unidentified. **Methods**: This study aims to identify these active compounds and evaluate the ability to inhibit the venomous potential of the four poisonous snakes by targeting PLA2, through *in silico* approaches. **Results:** The compounds aristolochic acid, aristolindiquinone, and ishwarol exhibited the highest binding affinity and established hydrogen bond interactions through molecular docking. Additional studies utilizing molecular dynamics simulations validated the stability of Aristolochic acid with the target proteins. **Conclusion:** Furthermore, aristolochic acid was extracted using the hot extraction method, followed by condensation and purification through silica gel column chromatography (60-120 mesh). The eluted fractions were then subjected to UV spectroscopy and HPLC analysis for preliminary confirmation of the compound.

Major Findings: *In silico* analysis demonstrated that aristolochic acid, aristolindiquinone, and ishwarol effectively inhibited PLA2 proteins from four venomous snake species, with aristolochic acid showing the highest stability during MD simulations. Ishwarol exhibited the strongest binding with PLA2 proteins of *Naja naja*, *Echis carinatus* and *Bungarus caeruleus*, while aristolindiquinone and aristolochic acid showed significant interactions with *Daboia russelii*.

Keywords: Aristolochic Acid, *A. indica* L., Molecular Simulation, Phospholipase A2, Snake Venom

1. Introduction

Snake envenomation is a critical medical condition and a significant health risk that results in a high number of fatalities, particularly in India[1]. It is one of the neglected tropical illnesses that primarily affects rural communities in tropical and subtropical nations[2]. However, based on data currently available

*Author for correspondence

Article Received on: 30.04.2025 Revised on: 24.06.2025 Accepted on: 10.07.2025

from the World Health Organization, between 4.5 and 5.4 million people are victimized by snakes each year. Of these, 81,000 to 138,000 people die from complications, and 1.8 to 2.7 million of them become clinically ill (WHO). Nearly 270 species with a spectrum of toxicity are likely to be noticed all over the country. 60 snake species are thought to be corrosive and can cause envenomation that is extremely dangerous. Among those the Krait (*B. caeruleus*), Russell's viper (*D. russelli*), Saw-scaled viper *(E. carinatus),* and Cobra *(N. naja)* are the four most common poisonous snakes found in nation[3]; The snake *N. naja, B. caeruleus* comes under the *Elapidae* family, and the snake *E. carinatus, D. russelli* comes under the *Viperidae* family. The sole type of medicine that can be effectively used to treat snakebite is antiserum. Consequently, according to WHO estimates, 80% of the world's population receives their main healthcare from conventional medicine[4]. In many countries, such as India, anti-venom therapy is only available at city headquarters. Since snakebites primarily occur on plantations in isolated areas, an inhibitor cocktail could be a very effective first-aid remedy[5]. Still, the vast majority of those living in rural and tribal areas persist in depending on indigenous herbal medicine systems for the majority of their health-related requirements, including the treatment of snake bites. Bioactive pharmacological compounds derived from medicinal plants can be directly utilized in the treatment of snakebite victims[6]. Among the many medicinal plants studied for snakebite treatment, *A. indica* L. is one of the most commonly used and significant species, traditionally employed by the Irula tribes[7]. The plant's *in vitro* antimicrobial, antifungal, anti-venomous, and antioxidant properties have already been investigated using crude and ethanolic extract[8]. Snake bite treatment is one of the many ailments for which the aqueous extract of *A. iaindica* L. roots is used as a decoction. Aqueous extract information is scarce, despite extensive research on the alcoholic extract of the plant's various parts[9]. The presence of several bioactive compounds in *A. indica* L. is well recognized, yet the specific metabolites that block the PLA2 enzyme have not been properly investigated or characterized. The crude extract of *A. indica* L. has been tested for antivenom efficacy against Phospholipase A2 (PLA2). However, to date, there is no evidence demonstrating antivenom activity from its isolated compounds. Alluvial, arid, and semi-arid regions of the Indian subcontinent are popular places to cultivate *A. indica* L., also known as Indian Birthwort. Utilizing various plant parts, such as leaves, stems, bark, and seeds[10]. The root is utilized most effectively as a beverage for treating bronchitis, asthma, ulcers, and insect and reptile bites[9]. Aristolindiquinone, aristololide, aristolochic acid, cephradione, aristolactum IIa, 2-hydroxy-1-methoxy-4 Hdibenzo quinoline- 4,5-(6H)-dione, stigmastenones II and III, aristolactam glycoside I, methylaristolate, ishwarol, ishwarone, β-sitosterol-β-D-glucoside, and aristolochene all have been identified as being present in *A. indica* L. roots[11,12]. In which the chemical constituents like aristolochic acid, aristolindiquinone, aristolochene, ishwarol, and ishwarol were reported to have antivenomous activity[13]. The venom of a snake is composed of many protein families, each of which has a wide variety of poisons or toxin isoforms. A single species of snake's venom usually comprises between 30 and over 100 protein/peptide poisons, many of which combine to increase the toxin's more dangerous[14]. The proteins in snake venoms are differentiated into 5 families: Dominant protein families, Secondary protein families, Minor protein families, Rare protein families, and Unique protein families, in which PLA_2 comes under the dominant protein families[15]. Because of its essential role in inducing an assortment of psychological responses in snakebite victims, phospholipase A2 is one among the most fascinating classes of proteins among snake venom enzymes[16]. Snake venom contains phospholipase A2 (PLA2), a multifunctional toxic enzyme responsible for delivering a wide range of toxic effects[17]. PLA2 catalyzes the hydrolysis of the sn-2 acyl ester bond in glycerophospholipids, which are key components of cell membranes and lipoproteins[18]. The 3 primary categories of venom found in snake PLA_2s are hemostasis-impairing toxins, myotoxins, and neurotoxins owing to the variety of toxic effects they exhibit. The current research is an attempt on computational study of 4 Indian venomous snakes using phytochemicals found in *A. indica* L.

roots through molecular docking and molecular dynamic studies. Additionally, the extraction of the compound aristolochic acid has been carried out.

2. Materials and Methods

2.1 *In Silico* Analysis

2.1.1 Protein Structure Retrieval

The crystalline structure of the target protein phospholipase A2 of 4 venomous snakes was retrieved from the RCSB Protein Data Bank using their PDB ID (Table 1). The target protein's downloaded structure was generated using the protein preparation wizard of the Schrodinger software (Schrodinger, LLC, New York, NY, 2018-3). The protonation state and optimization of H-bonding in the target proteins were assigned using protassign, and the structure was optimized using the 'impref' minimization tool for liquid simulations (OPLS 3e) force field of Schrodinger software. As the structures lack a co-crystallized ligand, the active site had been predicted using Sitemap.

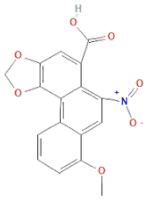
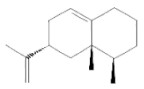
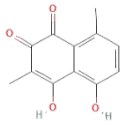
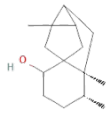
2.1.2 Retrieval of Ligands

Compounds ishwarol, aristolochene, ishwarone, aristolochic acid, and aristolindiquinone from the plant *A. indica* L. were reported to have anti-phospholipase A2 activity (Table 2)[13]. The 3D structures of the compounds known to have anti-snake venom properties have been downloaded in SDF format from the NCBI PubChem database. The LigPrep module in Schrodinger was used to create all the ligands, which were then employed in the workflow for molecular docking. The LigPrep tool is used to determine all-possible protonation and tautomeric states of ligands within a pH range of 7.0±2.0.

Table 1. Details of the experimental structures of the target protein phospholipase A2 from venomous snakes

Snake Species	PDB ID
D. russelli	2PYC
N. naja	1A3F
E. carinatus	2QHE
B. caerulus	1DPY

Table 2. Chemical structure of the ligands

S. No	Compound name	Compound ID	Structure of Compound
1	Aristolochic acid	2236	
2	Aristolochene	161533	
3	Aristolindiquinone	442723	
4	Ishwarone	15559789	
5	Ishwarol	42608203	

2.1.3 Molecular Docking Analysis

Insights gained from molecular docking analysis provide a fresh outlook on comprehending and validating our comprehension of protein-ligand interactions[19]. In this study, the phospholipase A2 (PLA2) proteins from 4 venomous snake species were subjected to molecular docking with 5 selected ligand structures. The docking process was conducted using the Glide module of Schrodinger software. The SiteMap module from Schrodinger was used to examine and predict the binding site in the protein. The 5 compounds that were chosen to inhibit the phospholipase of snake venom undergo molecular docking analysis with the PLA2 of the poisonous snakes through Induced Fit Docking (IFD)[20].

2.2 Molecular Dynamics Simulations

MD-simulation helps in analyzing the protein action of the Protein-Ligand Complex (PLC) at the target's binding site region under physiological conditions. Molecular Dynamics (MD) simulations were carried out using Maestro to evaluate the stability of the

ligand-protein complexes within the active site of PLA2. MD simulation was performed for the PLA2 of 4 poisonous snakes with the compounds that show the top scoring in the molecular docking analysis through IFD using the Desmond module of the Schrodinger Software. The system builder panel was used for creating the initial setup for the MD simulation. For the compounds screened using molecular docking procedures, the simulation ran for 100 ns. Configuring the initial system utilizing the system builder panel signified the initial stage of the MD simulation setup. Complexes were constructed within an orthorhombic box and immersed in SPC water models for salvation. System equilibration was then carried out using the NPT ensemble, adhering to default Desmond options. A 150ns production run ensued with a 2ps relaxation time. Throughout the simulation, a Martyna-Klein barostat (a) maintained a pressure of 1 atm, and a Nose-Hoover chain thermostat (b) regulated the system temperature at 300K[21,22].

2.3 Collection of Plant Material

Fresh roots of *A. indica* L. were collected from Kolli Hills, Namakkal District, Tamil Nadu, and the plant was identified and authenticated at the Botanical Survey of India, Coimbatore. The collected root samples of *A. indica* L. were shade dried, powdered and stored for further analysis.

2.4 Extraction of the Plant Material

Soxhlet extraction of root sample (20 g) was performed using methanol (300 mL) and the extract was finally condensed to 10 ml using rotary vacuum evaporator[23].

2.5 Methanolic Extract Fractionation by Column Chromatography

Methanolic extract (5 mL) of *A. indica* L. root samples were chromatographed on a silica-gel column of mesh size 60-120 using chloroform/methanol mixture (1:1 v/v) as mobile phase and the UV absorption of all the fractions was determined at 320 nm[24].

2.6 HPLC Analysis

The fractions were collected from the methanolic root extract of *A. indica* L. The obtained fractions were analyzed by UV-Vis spectroscopy followed by the HPLC analysis as the preliminary confirmation of the compound in the isolated extract. Agilent 6125B SQ LC/MSD, Mass detector with LC Stack for Open LAB ChemSta 1260 Quat Pump 600 bar, column oven, and auto samplers with UV-detector were used in order to assess the fractions. The HPLC injections were performed in the gradient method with the combination of mobile phase ranging from 5% to 95% of Water-Methanol for 20 minutes. Infinity Lab Agilent Poroshell 120 EC-C18 column size: 4.6 x 100 mm 2.7 micron was used with the flow rate of 0.5 mL per min. The injection volume of 10 µL was used and 2 wavelengths of 218 and 254 nm were used in the UV detector. The extracted fraction on 500 uL was checked for any precipitation and diluted to 1.5 mL of Carbinol (HPLC grade) was used, and a 0.2 micron filter was used for filtering. In order to inject the prepared sample, the HPLC sample plate was loaded.

3. Results

Molecular docking and molecular dynamics simulation were utilized as computational techniques. The inhibitory mechanism of the compounds Ishwarol, Aristolochene, Ishwarone, Aristolochic acid, and Aristolindiquinone were studied against the PLA2 of *D. russelli, N. naja, E. carinatus*, and *B. caerulus* using molecular docking. Furthermore, antivenom metabolite aristolochic acid was extracted from the roots of *A. aindica* L. The methanolic extract was further condensed to separate the desired component and was isolated using column chromatography.

3.1 Molecular Docking Analysis

Molecular docking serves as vital in determining the binding mechanism of a protein and the ligand it binds. The target-ligand interaction and the target enzyme's stability as well as its mechanistic action were identified through the *in-silico* methods. Several hydrogen bonds were identified in the docked complex in this research, indicating robust binding in the ligand-protein system. 5 compounds were docked with the 4 proteins of venomous snakes of India. To determine the precise binding modes, Induced Fit Model was performed. This algorithm ensures active site geometry accuracy by employing the

Table 3. Calculated dock score, prime energy, IFD score and hydrogen bonding details of the ligand with PLA2 of the snake *N. naja*

Snake Species	Protein ID	Ligand	No. of Hydrogen Bond	Docking Score	Prime Energy	IFD Score
N. naja	1A3F	Aristolochene	0	-8.469	-5474.24	-282.05
		Ishwarol	2	-8.821	-5383.84	-278.01
		Ishwarone	1	-8.627	-5409.66	-279.11
		Aristolindiquinone	2	-6.088	-5403.68	-278.61
		Aristolochic Acid	0	-6.149	-5408.12	-276.56

Glide and Prime programs to thoroughly consider all conceivable binding modes and corresponding conformational changes inside the receptor's active sites. The presence of hydrogen bonding is necessary for analyzing the specificity of protein-ligand interaction. They foster cellular functioning by enabling interactions between molecules. Ligand binding affinity is influenced by the proportion and positioning of hydrogen bond acceptors within the interaction interface.

The binding capability of the selected ligands was assessed by focusing on key parameters such as the docking score, prime energy, IFD score, and the number of hydrogen bonds. Lower docking scores indicate stronger binding. Ishwarol stands out with the lowest docking score of -8.821 kcal/mol, suggesting a robust interaction with the target protein PLA2. Aristolochene and Ishwarol also demonstrate a comparable docking score (-8.469 and -8.821 kcal/mol respectively), indicating its potential as a strong ligand. Bit higher scores than the above-mentioned compounds, aristolindiquinone and aristolochic acid also showed good docking scores of -6.088 and -6.149 kcal/mol respectively (Table 3). Additionally, it becomes obvious that all of the compounds exhibit promising IFD scores, which account for conformational changes inside the receptor's active site. Apart from these scores, the number of hydrogen bonds formed between ligands and proteins is a critical factor influencing the specificity and strength of the interactions. The compounds ishwarol and aristolindiquinone showed 2 hydrogen bond interactions each: With the residues TRY27 and GLY29 (Figure 1A) and HIE47 and, GLY29 respectively, suggesting strong interaction with the target. Apart from hydrogen bonding, aristolindiquinone also possesses pi-pi stacking interaction with the residue TRP18 (Figure 1B), which shows the protein-ligand binding specificity. These findings suggest that Ishwarol and Aristolindiquinone are promising candidates for further exploration as potential ligands targeting *N. naja* PLA2.

The docking results for the snake *B. caeruleus*-indicate that Ishwarol stands out with the least docking score of -8.442 kcal/mol, reflecting a strong interaction with PLA2, the target protein. Similar docking scores (-7.512 and -7.948 kcal/mol, respectively) for ishwarone and aristolindiquinone imply that they might function as efficient ligands as well. Additionally, the compounds aristolochene and aristolochic acid exhibited favourable docking scores of -6.925 and -6.656 kcal/mol, respectively (Table 4). Notably, aristolindiquinone displayed 4 interactions between hydrogen bonds and the residues LYS31, SER114, GLY26, SER114 (Figure 2A), along with a salt bridge interaction with the residue LYS31 (Figure 2B). These results depicted in Table 3 imply that aristolindiquinone is a good option for further investigation to see whether it can bind to *B. caeruleus* PLA2.

In the docking results for the snake *D. russelii*, the compounds aristolindiquinone and aristolochic acid exhibit the highest docking score of -11.428 and -11.372 kcal/mol, respectively, indicating a strong potential as ligands (Table 5). Aristolindiquinone showed 10 hydrogen bond interactions with the residues HIE48, ASH49, CYS29, GLY30, and LEU2 (Figure 3A). On the other hand, aristolochic acid showed 5 hydrogen interactions with the residues TRY22, SER23, SER24 along with pi-pi stacking interaction with PHE5 and HIE48 (Figure 3B). Additionally, ishwarol displayed a docking score of -10.034 kcal/mol, featuring 5 hydrogen bond interactions with the residues GYL30, HIE48, TYR28 and CYS50 (Figure 3C). These findings suggest the potential of these compounds as ligands for *D. russelii* PLA2.

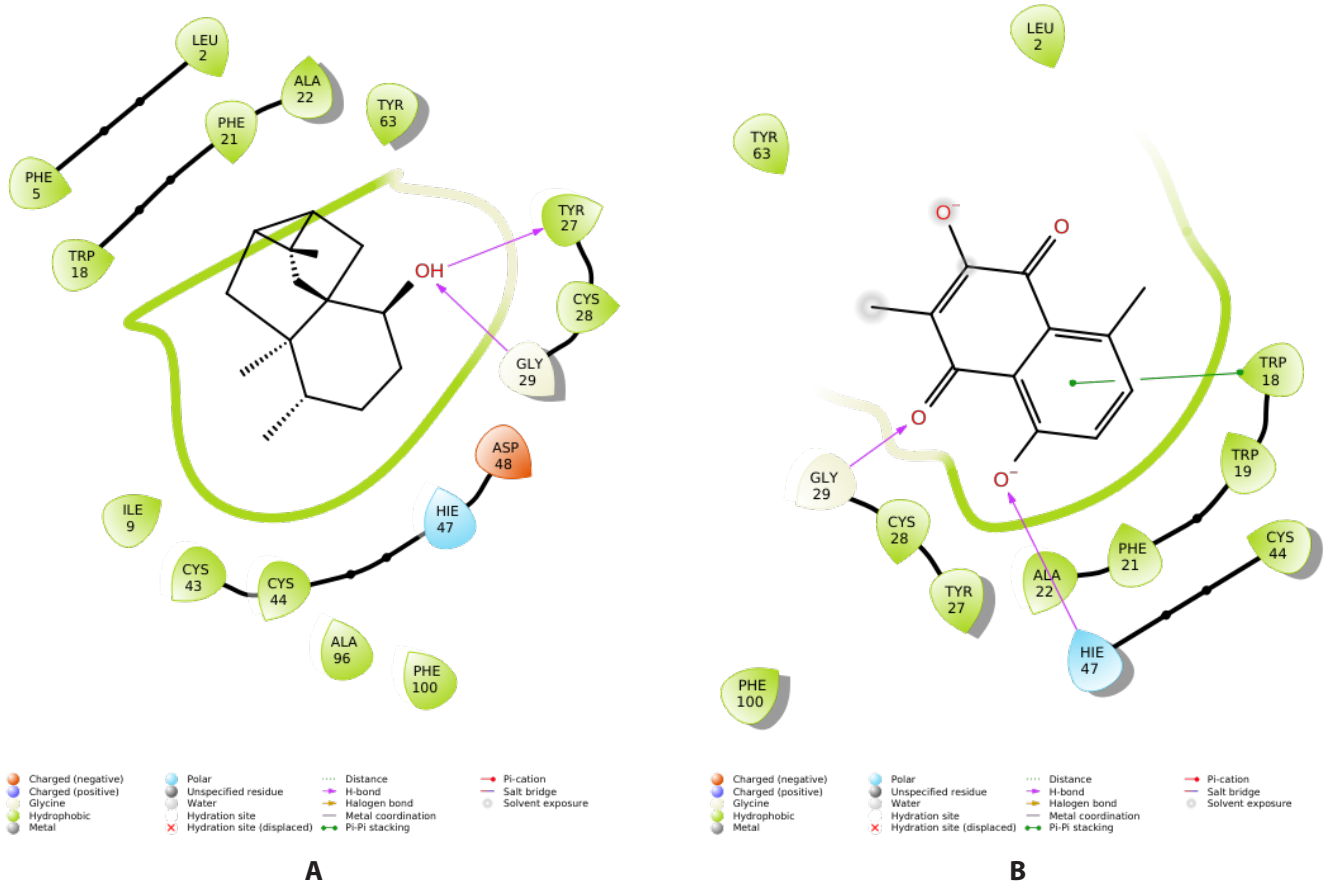


Figure 1. **(A).** Interaction of the compound Ishwarol with PLA2 of *N. naja;* (**B**). Interaction of the compound Aristolindiquinone with PLA2 of *N. naja*. **A**

Table 4. Calculated dock score, prime energy, IFD score and hydrogen bonding details of the ligand with PLA2 of the snake *B. caeruleus*

Snake Species	Protein ID	Ligand	No. of Hydrogen Bond	Docking Score	Prime Energy	IFD Score
B. caeruleus	1DPY	Aristolochene	0	-6.925	49675261.12	2483756.13
		Ishwarol	1	-8.442	49675320.9	2483757.6
		Ishwarone	1	-7.512	49675323.91	2483758.68
		Aristolindiquinone	4	-7.948	49675311.89	2483757.62
		Aristolochic Acid	1	-6.656	49675273.61	2483757.02

In the docking result for the snake *E. carinatus*, the compounds Ishwarol, Aristolochic acid and Ishwarone exhibited similar docking scores of -8.743,-8.376 and -8.274 kcal/mol respectively (Table 6). Additionally, each of these compounds displayed 2 hydrogen bond interactions, with Ishwarol interacting with the residues TYR22, and GLY30(Figure 4A). Ishwarone with GLY30, and GLY31 (Figure 4B) and Aristolochic acid interacting with the residues GLY30 and LYS69 (Figure 4C). These consistent docking scores and interactions suggest a comparable potential for ishwarol, aristolochic acid and ishwarone as ligands for *E. carinatus* PLA2.

Therefore, using the *in silico* approach, all the compounds exhibit an acceptable docking score, with the compounds aristolochic acid, aristolindiquinone, and ishwarol displaying higher docking scores and forming hydrogen bond interactions with all four proteins. These predominant interactions suggest that these compounds warrant further examination as potential candidates for therapeutic interventions.

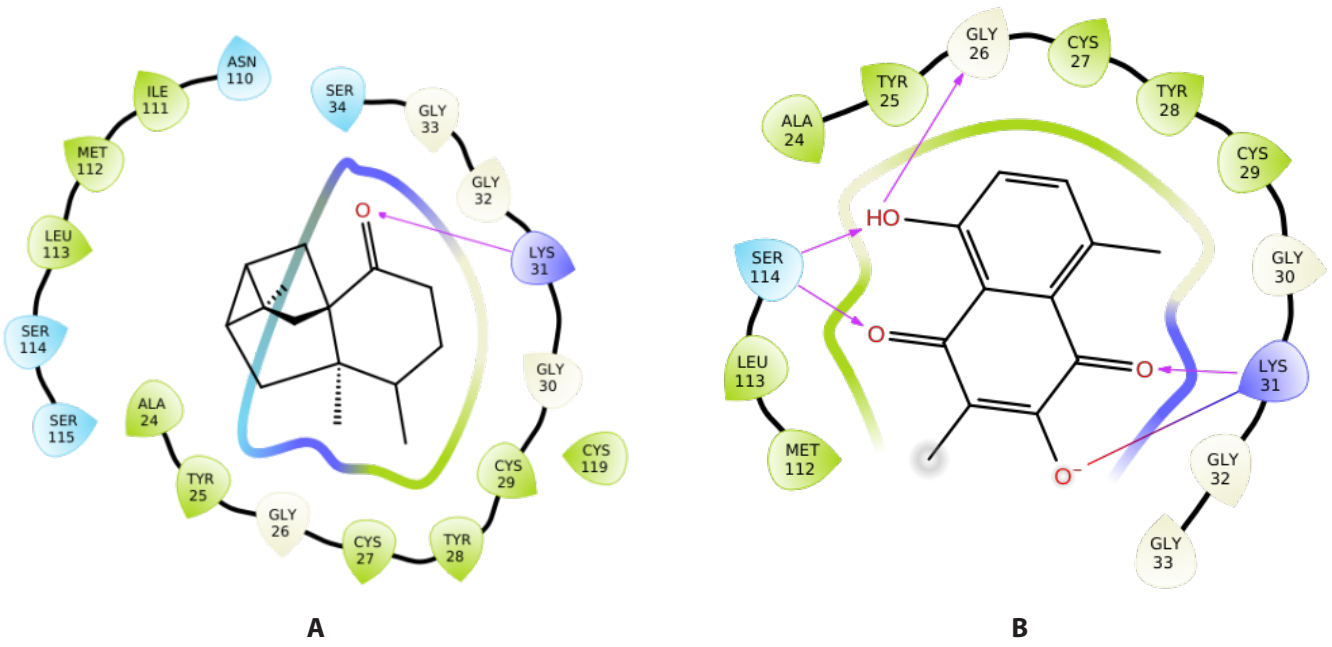


Figure 2. **(A).** Interaction of the compound Ishwarol with PLA2 of *B. caeruleus*; **(B).** Interaction of the compound Aristolindiquinone with PLA2 of *B. caeruleus*.

Table 5. Calculated dock score, prime energy, IFD score and hydrogen bonding details of the ligand with the PLA2 of the snake *D. russelii*

Snake Species	Protein ID	Ligand	No. of Hydrogen Bond	Docking Score	Prime Energy	IFD Score
D. russelii	2PYC	Aristolochene	0	-8.14	-5570.85	-286.68
		Ishwarol	5	-10.034	-5530.15	-286.54
		Ishwarone	3	-9.046	-5542.11	-286.15
		Aristolindiquinone	10	-11.428	-5564.13	-289.66
		Aristolochic acid	5	-11.372	-5537.27	-288.24

3.2 Molecular Dynamics Simulations

The significance of the interactions between ligands and amino acids was determined through molecular docking studies. The top complexes screened for various species were subjected to molecular dynamics simulations using Desmond module. Analysis of the optimal protein-ligand complexes, conducted over 100ns simulation time, provided insights into the stability and interactions of the molecules. This analysis was crucial for gaining insights into the interactions and stability, where the Root Mean Square Deviation (RMSD), Root Mean Square Fluctuation (RMSF), and the interaction plots were examined. The RMSD, indicating the deviation of the C from the original reference structure, was particularly instrumental in assessing the complexity of these deviations[25]. During the simulation, the ligand RMSD was monitored to assess the stability of the ligand within the binding pocket. The RMSF graph is utilized to elucidate the dynamic behavior of individual residues, providing insights into the protein's flexibility and potential functional implications. The top three compounds that showed the best docking score and hydrogen bonding against PLA2 of four poisonous snakes were identified as aristolochic acid, aristolindiquinone, and ishwarol. The investigation of these compounds and their corresponding targets is covered in more detail in subsequent sections.

3.2.1 MD Simulation of the Compound Aristolochic Acid with PLA2 of Four Poisonous Snakes

In the case of PLA2-Aristolochic acid, the protein exhibits minimal deviation throughout the simulation. The ligand exhibits a stable conformation during the

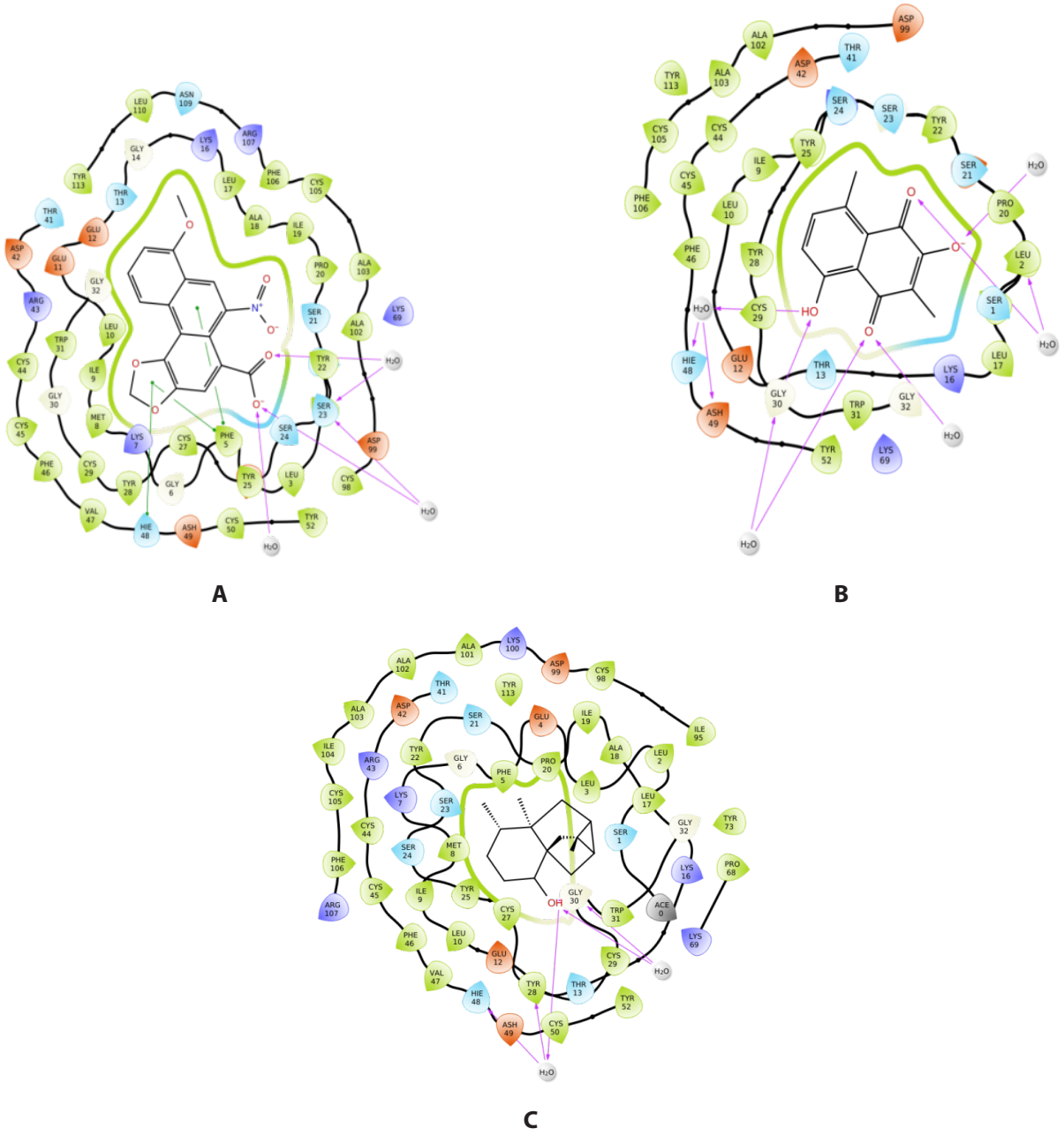


Figure 3. **(A).** Interaction of the compound Aristolochic acid with PLA2 of *D. russelli*; **(B).** Interaction of the compound Aristolindiquinone with PLA2 of *D. russellii*; **(C).** Interaction of the compound Ishwarol with PLA2 of *D. russelii*.

Table 6. Calculated dock score, prime energy, IFD score and hydrogen bonding details of the ligand with PLA2 of the snake *E. carinatus*

Snake Species	Protein ID	Ligand	No. of Hydrogen Bond	Docking Score	Prime Energy	IFD Score
E. carinatus	2QHE	Aristolochene	0	-7.543	54929.89	2738.95
		Ishwarol	2	-8.743	2074902651	103745123.8
		Ishwarone	2	-8.274	2074902586	103745121
		Aristolindiquinone	1	-7.27	2074902553	103745120.4
		Aristolochic Acid	2	-8.376	54901.19	2736.68

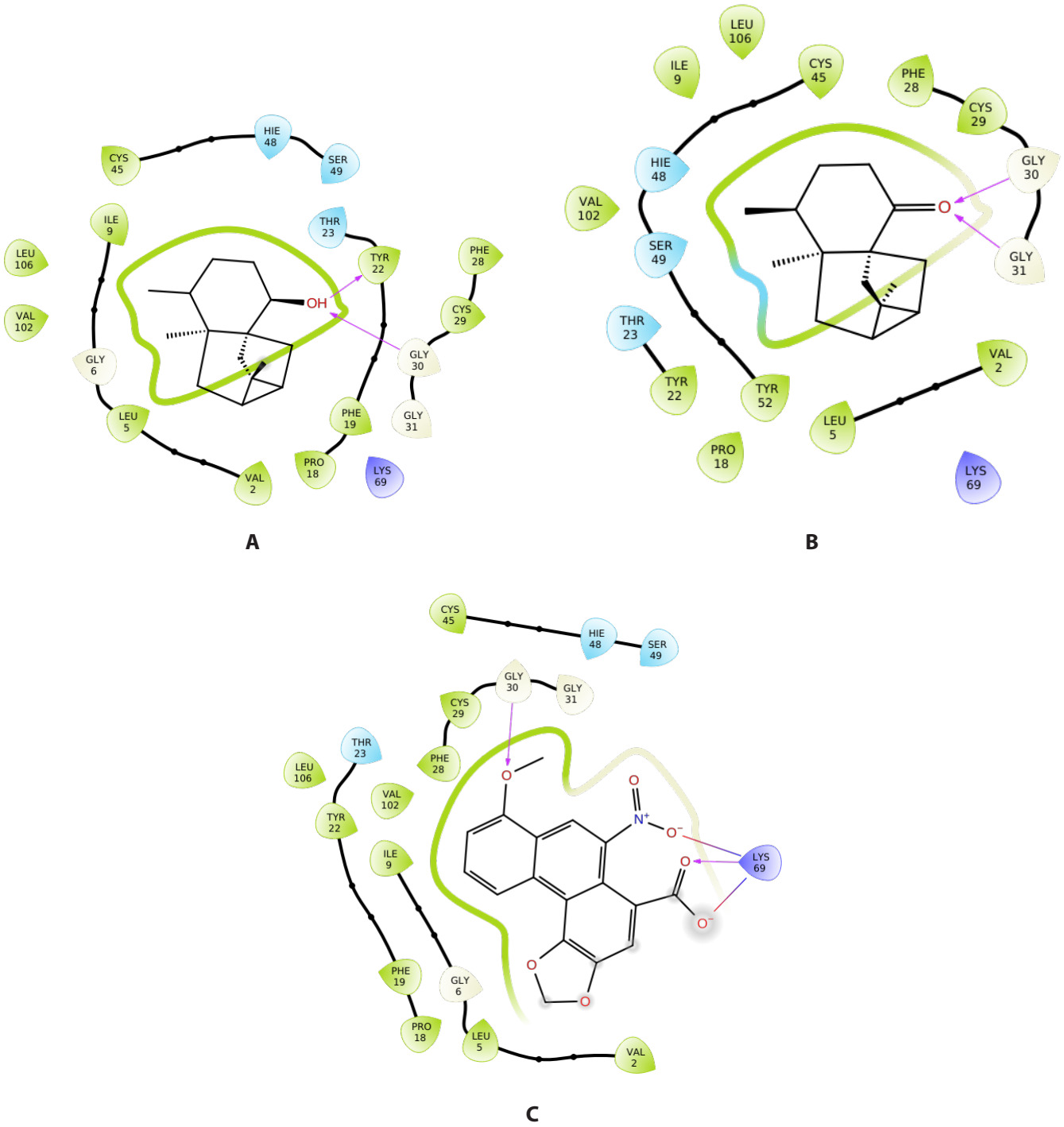


Figure 4. **(A).** Interaction of the compound Ishwarol with PLA2 of *E. carinatu;* **(B).** Interaction of the compound Ishwarone with PLA2 of *E. carinatus;* **(C).** Interaction of the compound Aristolochic acid with PLA2 of *E. carinatus.*

initial phase, whereas deviations were observed from 85 to 95ns, maintaining very minimal deviation until the end of the simulation. RMSF showed a more flexible peak between 40 and 100ns. The ligand in the *E. carinatus* contact exhibited a consistent increase in RMSD starting at 0.4A and remained flexible at 10ns. Both the ligand and the protein in the *B. caeruleus* snake's protein-ligand combination remained steady throughout the simulation.

Using aristolochic acid as the ligand for the RMSD graph in the context of the *N. naja* snake protein, the ligand initially maintains a stable conformation in the

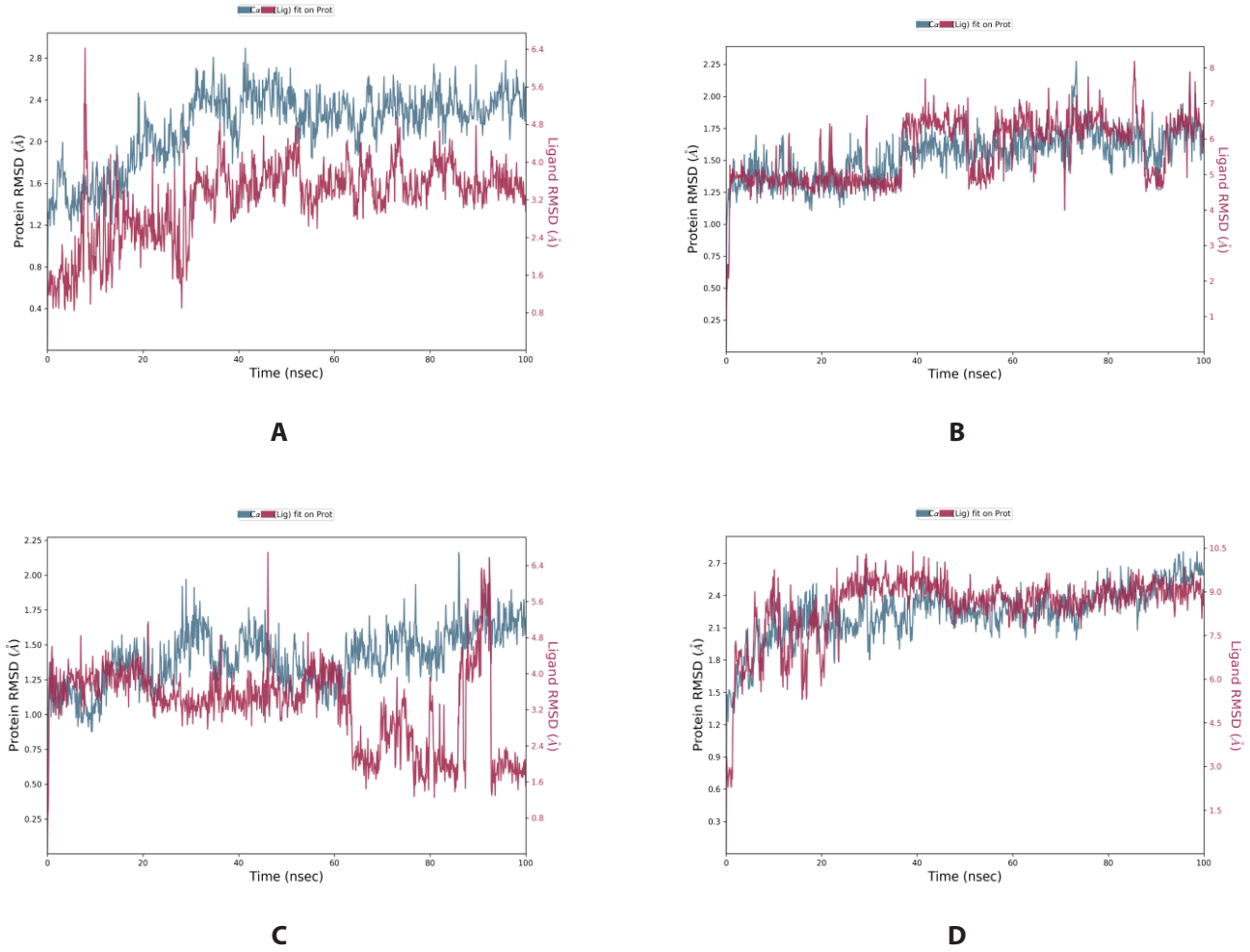


Figure 5. RMSD of PLA2 - Aristolochic acid complexes for **(A).** *N. naja*; **(B).** *D. russelli*; **(C).** *E. carinatus*; **(D).** *B. caeruleus*.

simulation's early phase (Figure 5A). Simultaneously, the protein demonstrates stability throughout the entire simulation, with a noticeable flexible peak observed between 40 and 100ns. In the instance of the *D. russelli* snake RMSD interaction, both the ligand and the protein exhibit increased flexibility over the 100ns simulation period (Figure 5B). In *E. carinatus* protein, the ligand consistently shows an increase in RMSD starting at 0.4 Å and remains flexible at 10ns (Figure 5C). For the protein-ligand combination in the *B. caeruleus* snake, both the ligand and the protein maintain stability throughout the entire simulation (Figure 5D).

We examined the Cα and ligand contacts to determine the amino acid residues interacting with the ligands throughout the MD simulation for Root Mean Square Fluctuations (RMSF) analysis. Every atom's fluctuation over the entire simulation is provided *via* RMSF. Using the ligand aristolochic acid, the RMSF of the proteins from the snakes *N. naja, D. russelli, B. caeruleus,* and *E. carinatus* was determined.

No significant fluctuations were observed, with only a minor fluctuation occurring at the 30th residue in comparison with the other regions, indicating a localized and relatively small deviation from the stable conformation at that site.

The 30th amino acid residue Tryptophan 18 the protein from the snake *N. naja* may possess more flexibility while interacting with residues, according to the RMSF (Figure 6A). The early phase of the *D. russelli* snake protein begins around 3.05° C, which is also the starting point for the residue interaction that gives the protein its flexibility (Figure 6B). The *E. carinatus* snake's protein appears to be quite flexible, with a residue index greater than 20-30ns (Figure 6C). The protein of the snake, *B. caeruleus*,

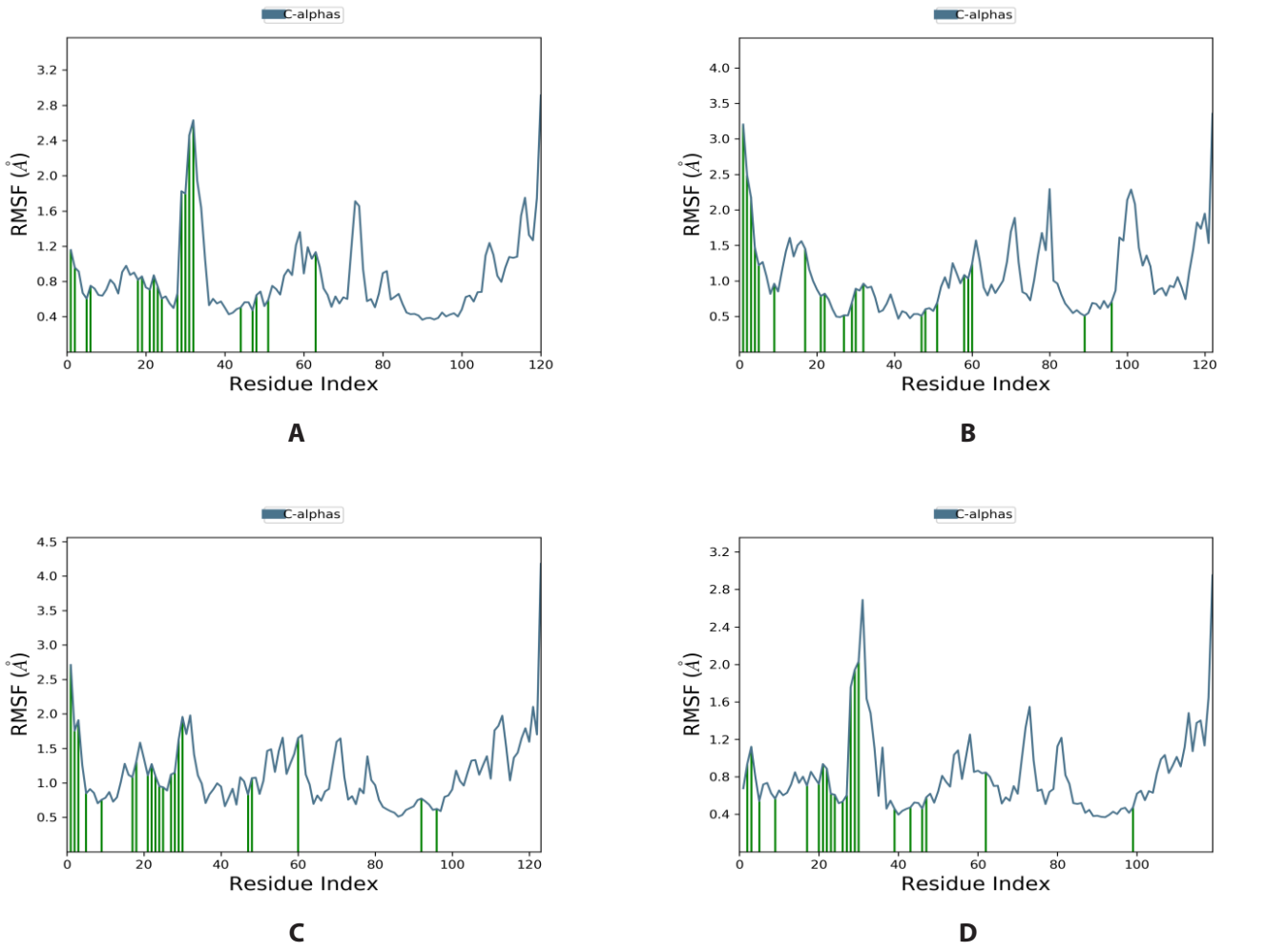


Figure 6. RMSF of PLA2 - Aristolochic acid complexes for **(A).** *N. naja*; **(B).** *D. russelli*; **(C).** *E. carinatus*; **(D).** *B. caeruleus.*

fluctuated by 2.7Å at 30ns (Figure 6D). Stability between the receptor and ligand was also assessed by examining interaction factors like hydrogen bonding, hydrophobic interactions, pi-pi cation interactions, and salt bridges, which were visualized through the simulation interaction diagram. The interaction plot for the ligand aristolochic acid with PLA2 of snake *N. naja* revealed three hydrogen bond interactions with the residues LYS6, TRP18, and ARG30 (Figure 7A). However, these interactions persisted for a limited simulation time, with an interaction fraction of approximately 0.5, which entails that, for the majority of the simulation, these interactions occurred. For the protein of the snake *D. russelli* showed 3 hydrogen bond interactions with the residues SER1, LEU2, and LYS69 (Figure 7B). For the protein of the snake *E. carinatus* showed 2 hydrogen bond interactions with the residue SER24 and TYR25 (Figure 7C).

3.2.2 MD Simulation of the Compound Aristolindiquinone with PLA2 of Four Poisonous Snakes

In the case of PLA2 with aristolindiquinone, when compared to their interactions in other snake species, the ligand displays the most variance during the simulation. The protein of the snake *N. naja* maintains stability with a very minimal deviation, starting with an RMSD of ~1.5Å and experiencing a very minor gradual increase until 38ns, after which it remains stable, indicating a relatively stable conformation. In contrast, the ligand demonstrates flexibility with an initial RMSD of around24Å, indicating a significant deviation from the initial binding pose. However, this is common as the ligand may undergo conformational changes or adjustments to find an energetically favorable binding mode. Moreover, a further decrease to around 12Å was observed. Both

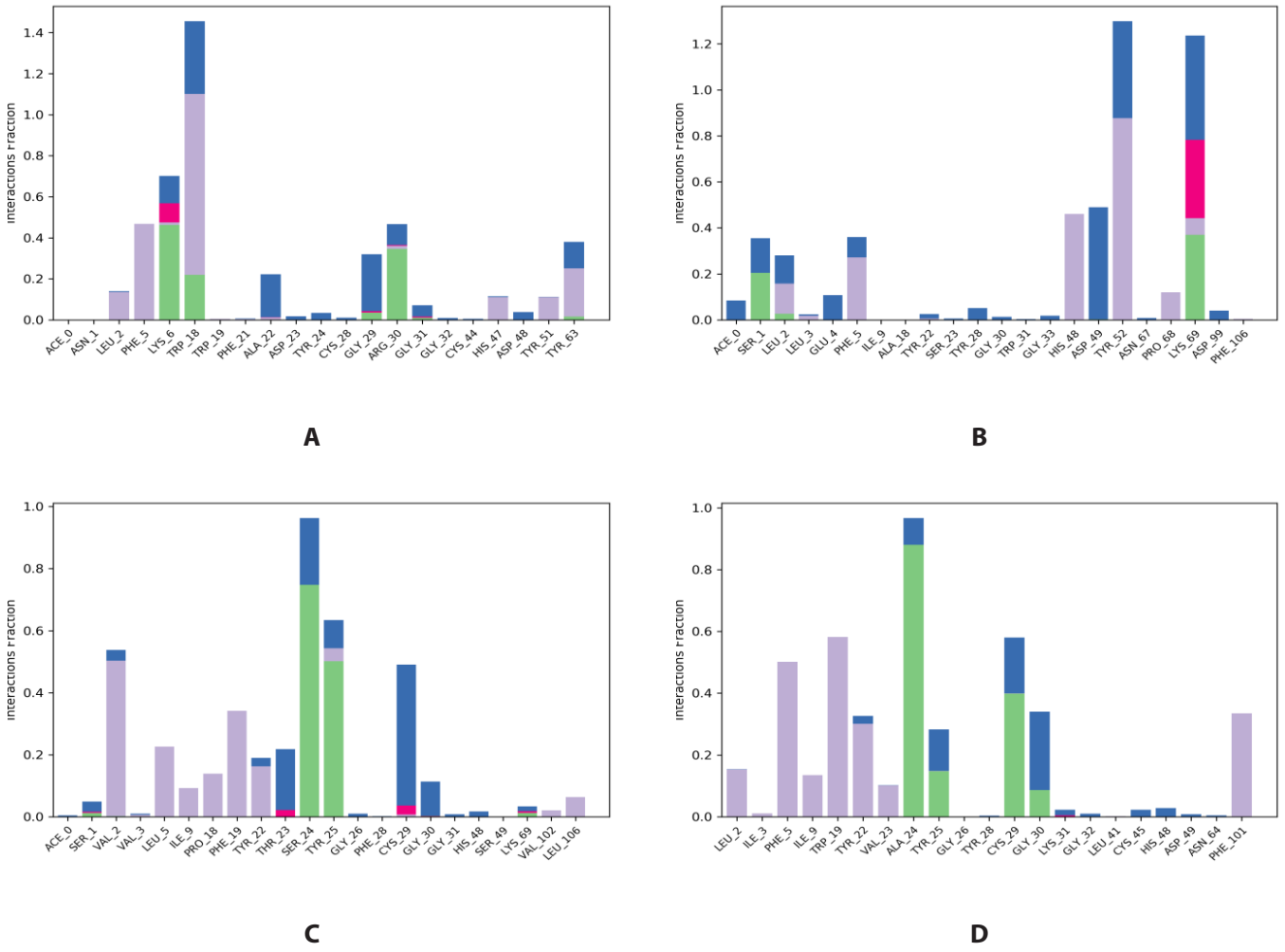


Figure 7. Interaction plot of PLA2 - aristolochic acid complexes for **(A).** *N. naja* **(B).** *D. russelli* **(C).** *E. carinatus* **(D).** *B. caeruleus.*

the protein and ligand undergo an initial structural adjustment followed by stabilization. The protein achieves stability with minor fluctuations, while the ligand settles into a stable binding pose and maintains this conformation throughout the simulation time (Figure 8A). Similarly, PLA2 of the snake *D. russelli* showed similar RMSD of *N. naja*. However, the ligand exhibited dynamic behavior, including initial conformational changes, transitions between different binding modes, and eventual stabilization with some fluctuations towards the end of the simulation. PLA2 from *B. caeruleus* exhibited deviations throughout the simulation but remained stable (Figure 8D). However, for the PLA2-Aristolindiquinone complex of the snake *E. carinatus*, both the protein and ligand were found to be stabilized throughout (Figure 8C). The RMSF plots indicate minimal fluctuations for most residues, with only a few showing minor deviations. Slight fluctuations, observed at the terminal residues could be attributed to the protein being exposed to the solvent environment (Figure 9A, 9B, 9C, 9D). Interaction plot for the ligand aristolindiquinone with PLA2 of snake *N. naja* showed 2 hydrogen bond interactions with the residue LYS6 and LYS10 (Figure 10A). Interaction plot for the snake *D. russelli* exhibited 10 hydrogen bond interactions with the residues SER1, LEU2, LEU3, GLY6, GLY30, ASN54, ASN67, LYS69, ASP71, ARG72 and LYS74 (Figure 10B). In case of snake *E. carinatus*, resulted in 2 hydrogen bond interactions were observed with the residues THR23, SER25, and CYS45 (Figure 10C). Similarly, for the interaction of the snake *B. caeruleus*, the interaction plot showed 2

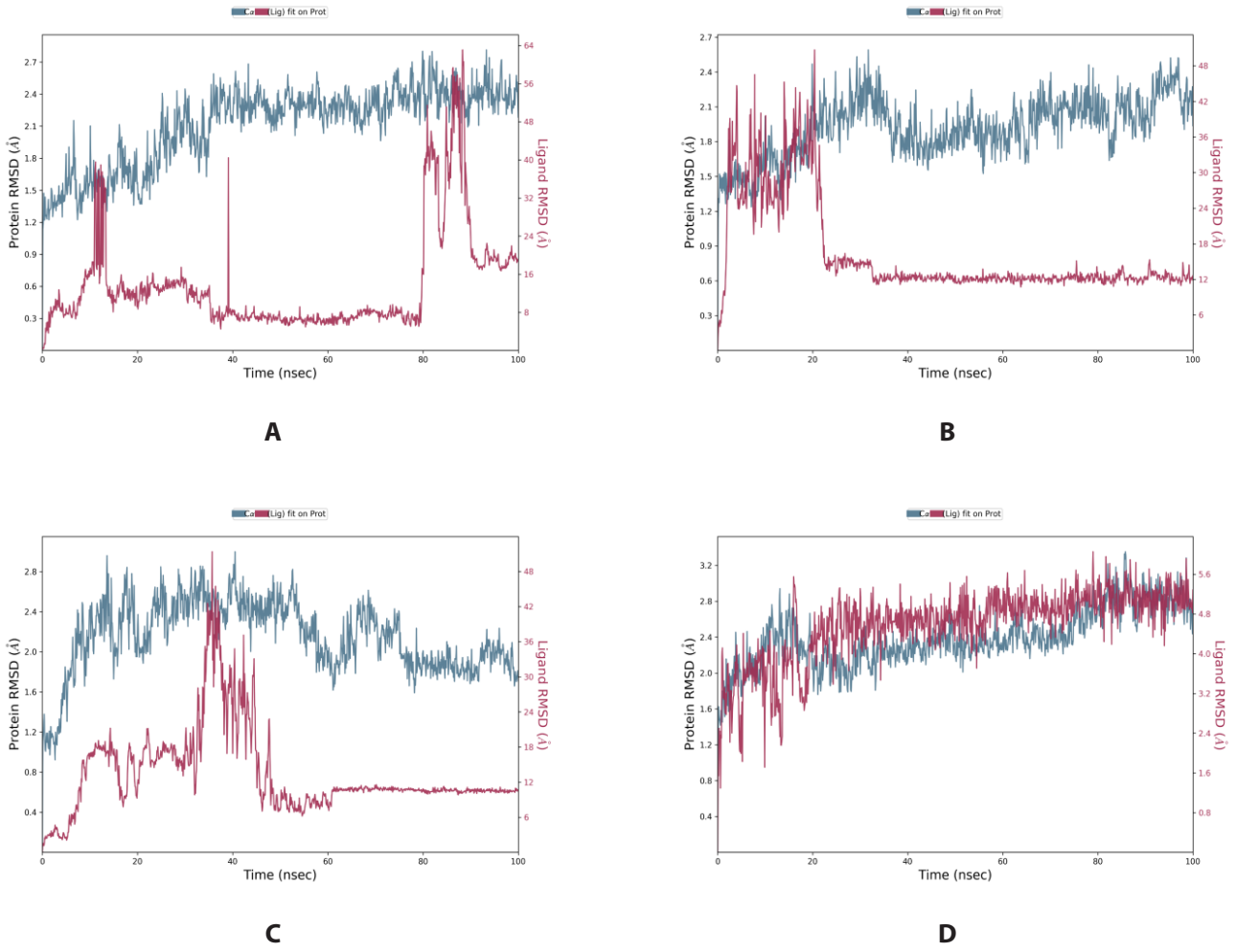


Figure 8. RMSD of PLA2 - aristolindiquinone complexes for **(A).** *N. naja*; **(B).** *D. russelli;* **(C).** *E. carinatus*; **(D).** *B. caeruleus.*

hydrogen bond interaction with the residues GLY30 and HIS48 (Figure 10D). In addition, ionic bonds and hydrophobic interactions were noted in addition to hydrogen bonds.

3.2.3 MD Simulation of the Compound Ishwarol with PLA2 of Four Poisonous Snakes

In the case of PLA2 interaction with ishwarol, the protein of the snake *N. naja* remained stable from the initial phase until the end (Figure 11A). The ligand interaction with the protein of the snake *D. russelli* was observed to be stable till 25ns followed by a major deviation for few numbers then resulted to be stable throughout (Figure 11B). The protein RMSD maintained a consistent pattern for *N. naja*, *D. russelli*, and *E. carinatus*. However, *B. caeruleus* exhibited a distinct pattern, corresponding with its interaction with aristolindiquinone (Figure 11D). Upon ligand binding, RMSF did not exhibit any significant fluctuations with *N. naja*, *D. russelli* and *E. carinatus* except for terminal residues. In contrast, *B. caeruleus* exhibited fluctuations, particularly notable with the 60th residue reaching approximately 4.2 Å (Figure 12D). This suggests that this particular residue might be more flexible or undergo conformational changes upon ligand binding, possibly due to alterations in the protein structure induced by binding. Interaction plot for the ligand ishwarol with PLA2 of snake *N. naja* reported four interactions between hydrogen bonds with the residues PHY21, ALA22, TYR27, GLY29 and HYS47 (Figure 13A). In the case of snake *D. russelli*, the interaction plot revealed 6 hydrogen bond

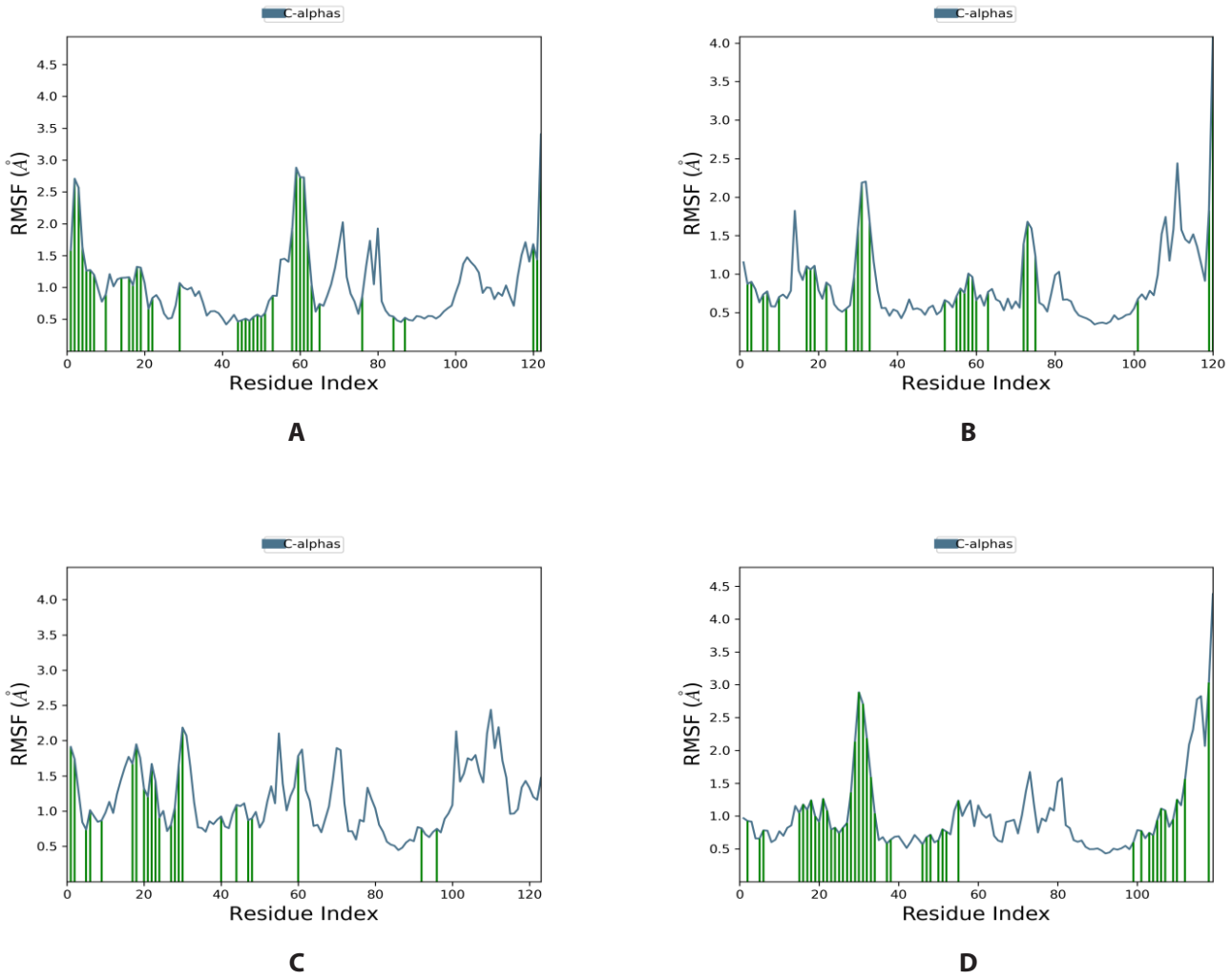


Figure 9. RMSF of PLA2- aristolindiquinone complexes for **(A).** *N. naja*; **(B).** *D. russelli*; **(C).** *E. carinatus*; (**D).** *B. caeruleus.*

interactions with the residues TYR22, TYR28, CYS29, GLY36, CYS45 and ASP49 (Figure 13B). Similarly, for the snake *E. carinatus*, 6 hydrogen bond interaction were observed with the residues VAL2, TYR22, THR23, CYS29, GLY30, and HIS48 (Figure 13C). The interaction plot forthe snake *B. caeruleus*, resulted more than 10 hydrogen bond interactions, with the residues LYS6, ASN7, GLN10, ARG17, LYS31, THR67, TYR106 and more (Figure 13D).

To verify the stable interactions acquired through dockingdata during the simulation, the hydrogen bonds, salt bridges, and hydrophobic interactions were computed and evaluated. Even though the complexes displayed more hydrogen bonds, some of which were discovered to have vanished or weaken during the simulation.

3.3 Extraction of Aristolochic Acid

Aristolochic acid was extracted from the roots of *A. indica* L. using a hot extraction method in a Soxhlet apparatus with methanol as the solvent. The methanolic root extract solvent was condensed using a rotary vacuum evaporator to 10ml. Further purification of the compound was performed with silica gel column chromatography.

3.4 UV-Visible Spectroscopy

Silica gel column chromatography was performed, and a total of 18 fractions, each of 10 ml, were collected. he collected fractions were analyzed using a UV spectrophotometer at 320 nm to detect the presence of the target compound. Fraction No. 6 exhibited the highest Optical Density (OD)

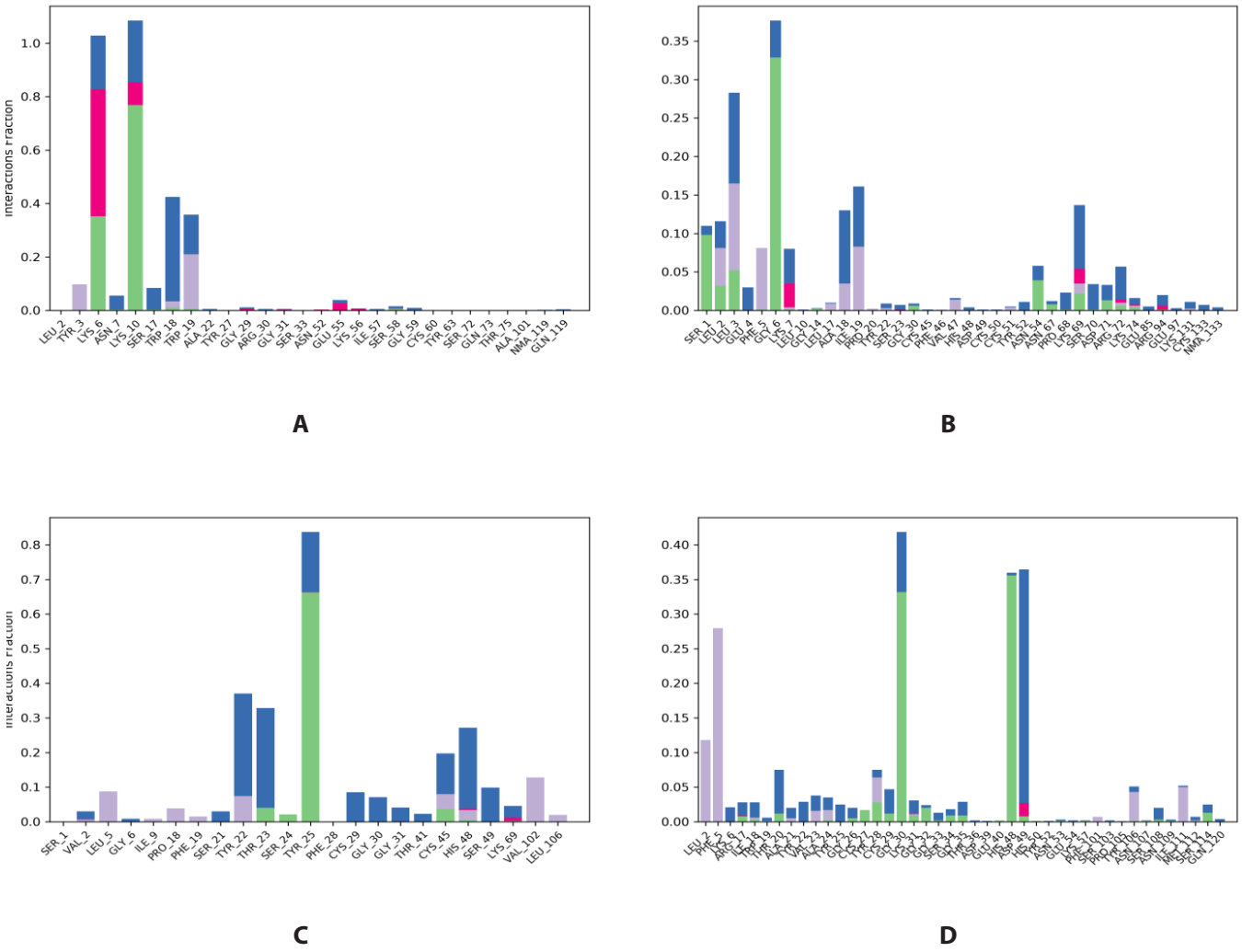


Figure 10. Interaction Plot of PLA2- aristolindiquinone complexes for **(A).** *N. naja*; **(B).** *D. russelli*; **(C).** *E. carinatus*; **(D).** *B. caeruleus*.

value of 2.2895 and was subsequently subjected to HPLC analysis to confirm the presence of the eluted compound.

3.5 HPLC Analysis of the Compound Aristolochic Acid

In this study, the presence of aristolochic acid in the eluted column fraction of *A. indica* L. methanol extract was identified by High-Performance Liquid Chromatography as shown in Figure 14A and B. As the desired compound, aristolochic acid is a highly polar compound, the peak eluted at 2.167 minutes corresponds to the high polar compounds in the reverse phase column in both wavelengths of UV of 218 nm and 254 nm. The presence of highly polar- OH functional groups in the molecular structure of aristolochic acid, as well as in the methanolic root extract of *A. indica* L., resulted in a chromatogram showing predominantly high-polarity elution. This observation confirms the presence of aristolochic acid in the extract.

4. Discussion

The aim of the study is to demonstrate that natural plant-based products and medicinal plants possess anti-venomous properties. The roots of *A. indica* L. contain chemical components such as ishwarone, aristolochene, ishwarol, aristolinidquinone, and aristolochic acid which have anti-snake venomous effects[9]. Additionally, this work showcases the

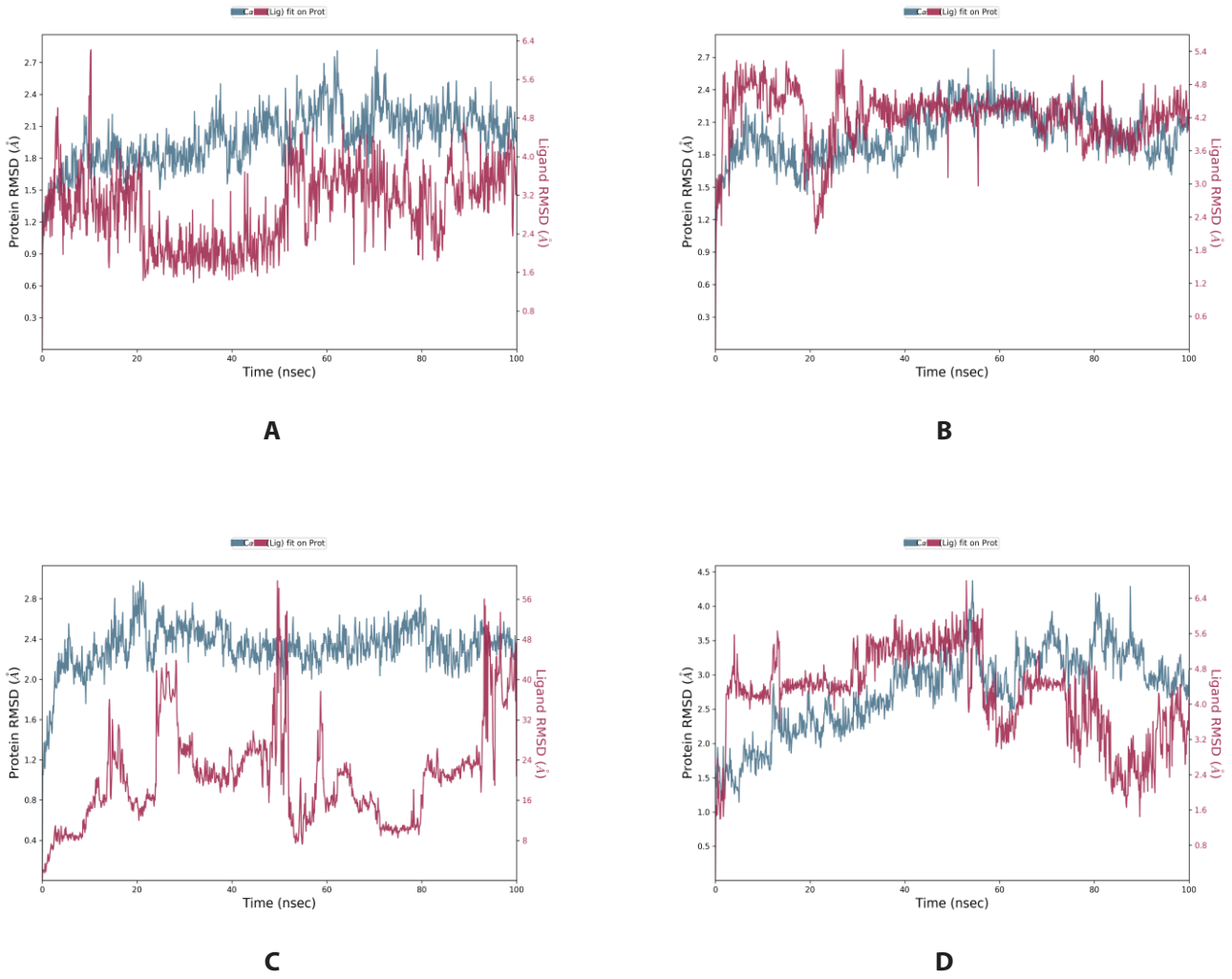


Figure 11. RMSD of PLA2- ishwarol complexes for **(A).** *N. naja*; **(B).** *D. russelli*; **(C).** *E. carinatus*; **(D)** *B. caeruleus*.

specific chemical that effectively inhibits PLA2. *In silico* analysis of the PLA2 proteins from four venomous snake species with 5 selected compounds suggests that aristolochic acid, aristolindiquinone, and ishwarol have the potential to act as effective inhibitors. Among the 5 compounds aristolochic acid, aristolindiquinone, aristolochene, ishwarol, and ishwarone interact with the PLA2 protein of the venomous snakes, the compound ishwarol shows the highest binding while interacting with the PLA2 protein of the snake's *N. naja*, *E. carinatus*, and *B. caeruleus* with 2, 2, and 1 hydrogen bond interaction respectively. The compound aristolindiquinine and aristolochic acid show more binding energy and hydrogen bond interactions with the PLA2 protein of the snake *D. russelli* with 10 and 5 hydrogen interactions respectively. MD simulation was performed for the 3 compounds aristolochic acid, aristolindiquinone, and ishwarol with all the proteins of the venomous snakes from which aristolochic acid resulted to be more stable compared with the other compounds. Notably, the aristolochic acid demonstrated stability across all the complexes, despite variations observed among species, particularly fluctuating in its binding with PLA2 of *E. carinatus*. However, ligand fluctuations can be acceptable, as they undergo conformational change or a transition to a different binding mode. Both ishwarol and aristolindiquinone exhibited numerous hydrogen-bonded interactions and binding energy and were found to be stable during the MD simulation, however, the nature of the ligand was found to be flexible. Hence, the extraction

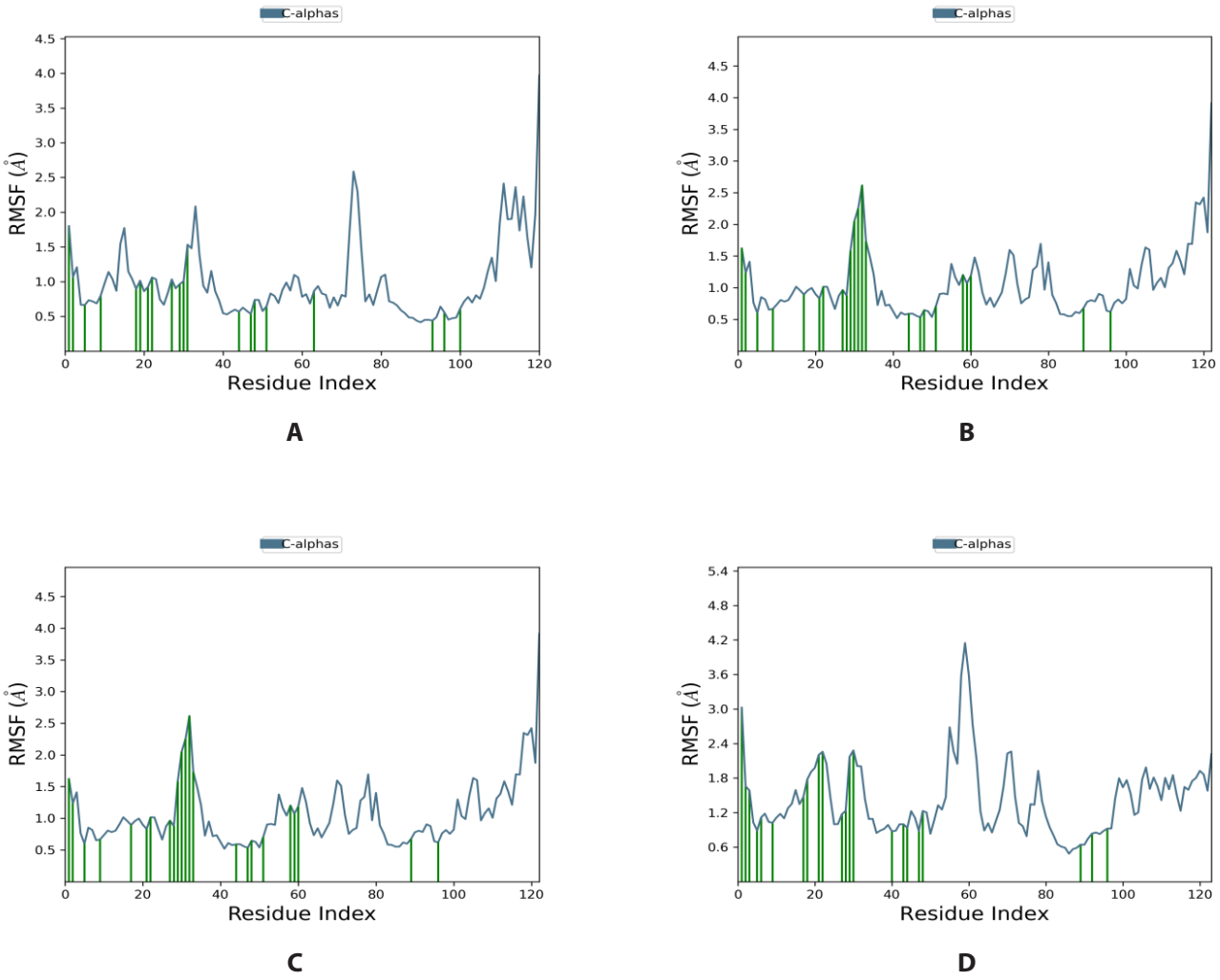


Figure 12. RMSF of PLA2- ishwarol complexes for **(A).** *N. naja*; **(B).** *D. russelli*; **(C).** *E. carinatus*; **(D).** *B. caeruleus*.

process of the compound aristolochic acid was prioritized. But according to current research, flexible molecules can also possess promising druggable potential, the other compounds may be considered for future research. The extraction of the compound from the roots was done with the methanol solvent, and the column was packed with silica gel to purify the compound[23,24]. Subsequently, the fractions can be analyzed using IR and NMR spectroscopy for structural characterization.

5. Conclusion

Based on the observations made in this study, the compound aristolindiquinone, aristolochic acid, and ishwarol possess good interaction with PLA2 enzymes, providing evidence for its potential to act as an anti-snake venom compounds. Simulation studies showed that aristolochic acid was significantly more stable than ishwarol and aristolindiquinone. From the results of the computational study, the compound Aristolochic acid was extracted from the roots of the plant *A. indica* L. and purified through column chromatography. Additional scientific investigation involving *in vitro* and *in vivo* studies is required to fully ascertain the effectiveness of the compound's effectiveness against the PLA2 enzyme of snake venom. Furthermore, investigating its mechanism of action and potential synergistic effects with existing anti-snake venom therapies could provide valuable insights for its development as a novel therapeutic agent against snake envenomation.

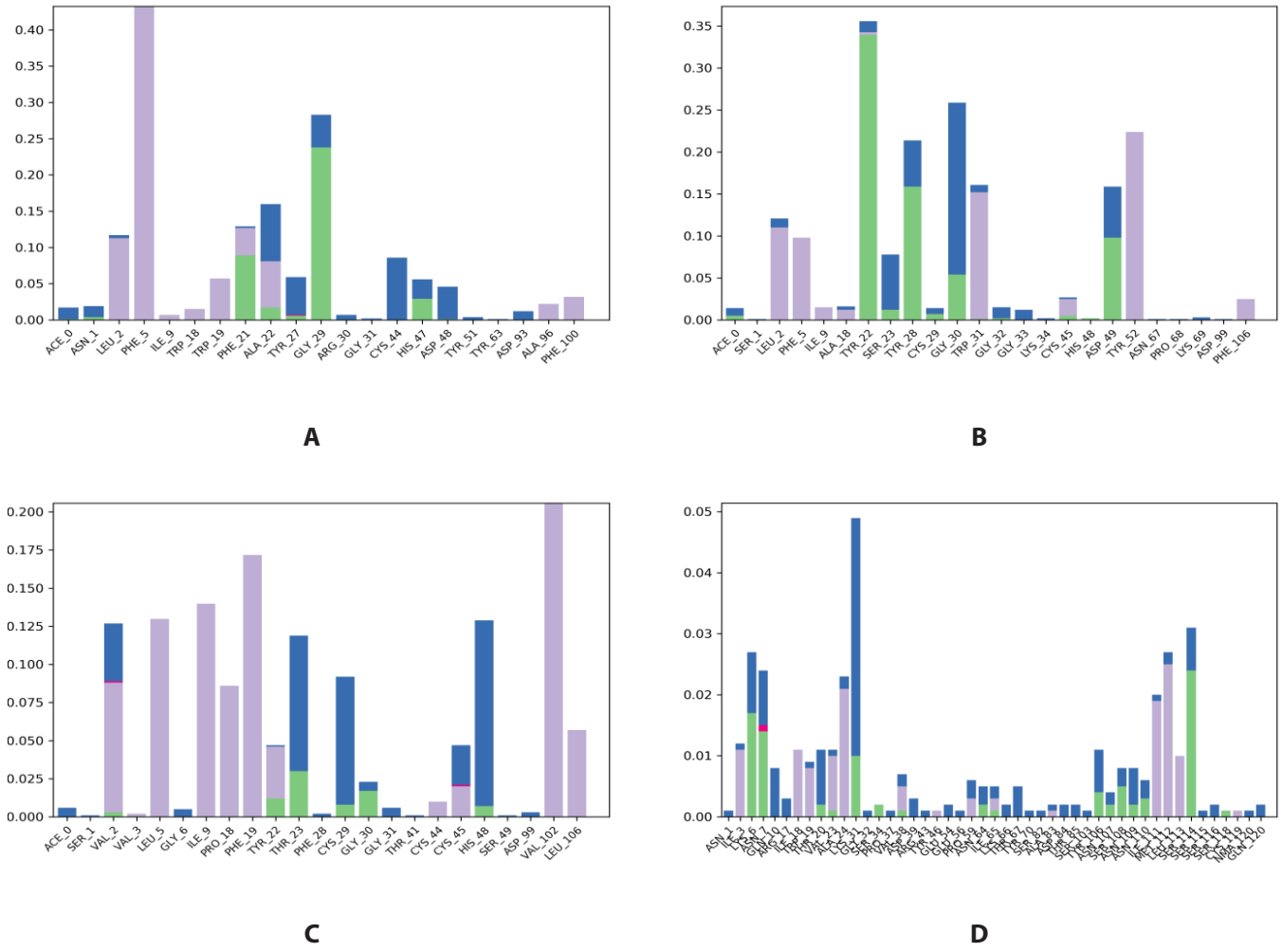


Figure 13. Interaction Plot of PLA2- ishwarol complexes for **(A).** *N. naja*; **(B).** *D. russelli*; **(C).** *E. carinatus*; **(D).** *B. caeruleus*.

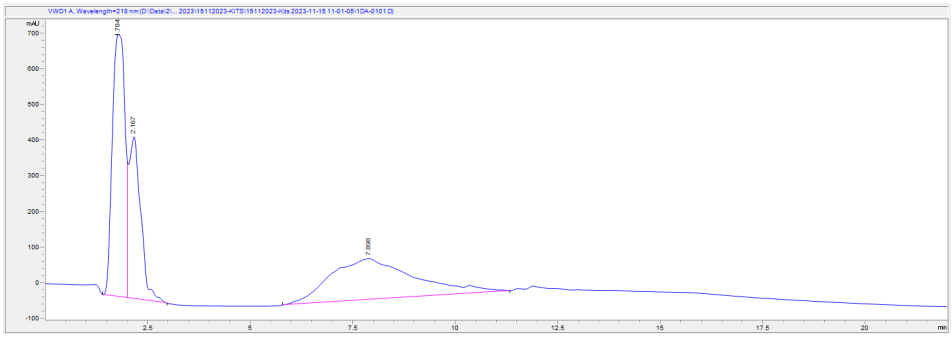


Figure 14. **(A)** HPLC chromatogram of isolated aristolochic acid from the methanolic extract of *A. indica* L. at 218 nm.

6. Author Contributions

Conceptualization, methodology, validation, *in-silico* software analysis, validation, investigation, writing original draft preparation- David Paul Raj R.S., Andrea Bernice W, *In silico* analysis software analysis- Beutline Malgija M, Kavinila S, Jannet Vennila J, validation, investigation- Jebasingh B and Premnath D. All authors have read and agreed to the published version of the manuscript.

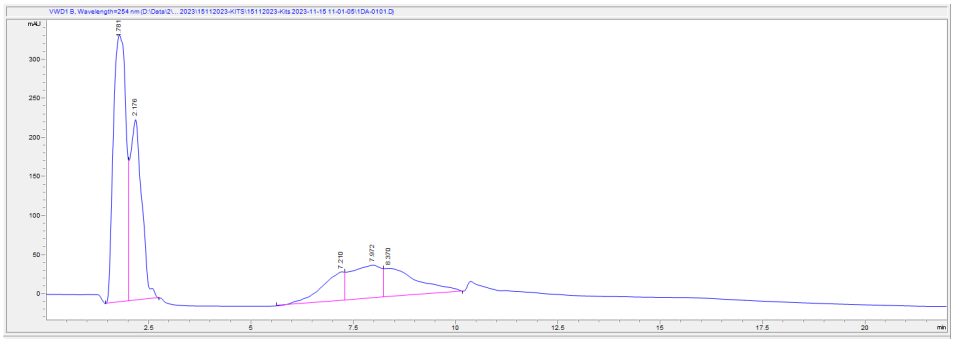


Figure 14. **(B)** HPLC chromatogram of isolated aristolochic acid from the methanolic extract of *A. indica* L. at 254 nm.

7. Acknowledgements

We thank Karunya Institute of Technology and Sciences, Coimbatore for providing infrastructure and laboratory.

8. References

1. Senthilkumaran S, Almeida RJ, Williams J, Williams HF, Thirumalaikolundusubramanian P, Patel K, *et al.* Rapid identification of bilateral adrenal and pituitary haemorrhages induced by Russell's viper envenomation results in positive patient outcome. 2023; 225:107068. https://doi.org/10.1016/j.toxicon.2023.107068
2. Rijal P, Singh AP, Panwar P, Pathania M, Kant R. Case report prolonged asymptomatic venom induced consumption coagulopathy : Caused by hemotoxic snake bite. 2022; 7448-7451.
3. Raj RSDP, Mathew AA, Jesse TJ, Kanimozhi RB, Preethy HA. Herbs as antidote for snakebite treatment in India- Traditional practices and it's future prospects - A review. J Nat Remedies. 2022; 22(3):269-290. https://doi.org/10.18311/jnr/2022/28405
4. Parveen A, Parveen B, Parveen R, Ahmad S. Challenges and guidelines for clinical trial of herbal drugs. J Pharm Bioallied Sci. 2015; 7(4):329-333. PMCID: PMC4678978. PMID: 26681895. https://doi.org/10.4103/0975-7406.168035
5. Girish KS, Kemparaju K. Inhibition of *Naja naja* venom hyaluronidase : Role in the management of poisonous bite. 2006; 78(13):1433-1440. PMID: 16253285. https://doi.org/10.1016/j.lfs.2005.07.015
6. Singh P, Yasir M, Hazarika R, Sugunan S, Shrivastava R. A review on venom enzymes neutralizing ability of secondary metabolites from medicinal plants. J Pharmacopuncture. 2017; 20(3):173-178. PMID: 30087793. PMCID: PMC5633669. https://doi.org/ 10.3831/KPI.2017.20.020
7. Michl J, Jennings HM, Kite GC, Ingrouille MJ, Simmonds MS, Heinrich M. Is aristolochic acid nephropathy a widespread problem in developing countries ? A case study of *Aristolochia indica* L . in Bangladesh using an ethnobotanical- phytochemical approach. J Ethnopharmacol. 2013; 149(1):235-244. https://doi.org/10.1016/j.jep.2013.06.028
8. Binorkar S, Parlikar G, Sawant R, Bhoyar M, Nikumbh MB. *In-vitro* trial of roots of Ishwarmuli (*Aristolochia indica* Linn.) for anti-microbial, anti-fungal and anti-oxidant activity. Int J Ayurvedic Med. 2020; 11(3):405-409. https://doi.org/10.47552/ijam.v11i3.1637
9. Bhattacharjee P, Bhattacharyya D. Characterization of the aqueous extract of the root of *Aristolochia indica*: Evaluation of its traditional use as an antidote for snake bites. J Ethnopharmacol. 2013; 145(1):220-226. https://doi.org/10.1016/j.jep.2012.10.056
10. Modak BK, Gorai P, Pandey DK, Dey A, Malik T. An evidence based efficacy and safety assessment of the ethnobiologicals against poisonous and non-poisonous bites used by the tribals of three westernmost districts of West Bengal , India : Anti-phospholipase A2 and genotoxic effects. Plos One. 2020; 15(11):e0242944. https://doi.org/10.1371/journal.pone.0242944
11. Dey A, Hazra AK, Mukherjee A, Nandy S, Pandey DK. Chemotaxonomy of the ethnic antidote *Aristolochia indica* for aristolochic acid content: Implications of anti-phospholipase activity and genotoxicity study. J Ethnopharmacol. 2021; 266:113416. https://doi.org/10.1016/j.jep.2020.113416
12. Padhy GK. A review of *Aristolochia indica*: Ethnomedicinal uses, phytochemistry, pharmacological and toxicological effects. Curr Tradit Med. 2021; 7(3):372-386. https://doi.org/10.2174/2215083806666200831173828
13. Sivaraj D, Shanmugam S, Rajan M, Sasidharan SP, Sathyanarayanan S, Muniyandi K, *et al.* Evaluation of *Aristolochia indica* L. and *Piper nigrum* L. methanol extract against centipede *Scolopendra moristans* L. using Wistar albino rats and screening of bioactive compounds by high pressure liquid chromatography: A polyherbal formulation. Biomed Pharmacother. 2018; 97:1603-1612. https://doi.org/10.1016/j.biopha.2017.11.114

14. Fernández ML, Quartino PY, Arce-Bejarano R, Fernández J, Camacho LF, Gutiérrez JM, *et al*. Intravascular hemolysis induced by phospholipases A(2) from the venom of the Eastern coral snake, *Micrurus fulvius*: Functional profiles of hemolytic and non-hemolytic isoforms. Toxicol Lett. 2018; 286:39–47.
15. Tasoulis T, Isbister GK. A review and database of snake venom proteomes. Toxins (Basel). 2017; 9(9):290. PMID: 28927001. PMCID: PMC5618223. https://doi.org/10.3390/toxins9090290
16. Xiao H, Pan H, Liao K, Yang M, Huang C. Snake venom PLA2, a promising target for broad-spectrum antivenom drug development. Biomed Res Int. 2017; 2017:6592820. PMID: 29318152. PMCID: PMC5727668. https://doi.org/10.1155/2017/6592820
17. Montecucco C, Gutierrez JM, Lomonte B. Cellular pathology induced by snake venom phospholipase A2 myotoxins and neurotoxins : Common aspects of their mechanisms of action. Cell Mol Life Sci. 2008; 65(18):2897-2912. PMID: 18563294. PMCID: PMC11131735. https://doi.org/10.1007/s00018-008-8113-3
18. Wang Y, Zhang J, Zhang D, Xiao H, Huang C, Xiong S. Exploration of the inhibitory potential of varespladib for snakebite envenomation. Molecules. 2018; 23(2):391. PMID: 29439513. PMCID: PMC6017252. https://doi.org/10.3390/molecules23020391
19. Dinesh TV, Malgija B, Ponraj MR, Muralakar P, Thathapudi JJ, Kandasamy R, *et al*. International journal of biological macromolecules design of novel pyrimidine based remdesivir analogues with dual target specificity for SARS CoV-2 : A computational approach. Int J Biol Macromol. 2023; 242(Part 1):124443. PMID: 37148943. PMCID: PMC10158044. https://doi.org/10.1016/j.ijbiomac.2023.124443
20. Mahmud S, Md. Rimon P, Yasir Mohamed R, Khaled Mahmud S, Suvendu R, Fahmida Alam T, *et al*. Exploring the potent inhibitors and binding modes of phospholipase A2 through in silico investigation. J Biomol Struct Dyn. 2020; 38(14):4221–31. https://doi.org/10.1080/07391102.2019.1680440
21. Martyna GJ, Klein ML, Tuckerman M. Nose- Hoover chains : The canonical ensemble *via* continuous dynamics Nose-Hoover chains : The canonical ensemble via continuous dynamics. J Chem Phys. 1992; 97(4):2635-2643. https://doi.org/10.1063/1.463940
22. Martyna GJ, Tobias DJ, Klein ML. Constant pressure molecular dynamics algorithms. J Chem Phys. 1994; 101:4177-4189. https://doi.org/10.1063/1.467468
23. Pradeepa V, Narayanan SS, Kirubakaran SA, Thanigaivel A, Nathan SS. Toxicity of aristolochic acids isolated from *Aristolochia indica* Linn (*Aristolochiaceae*) against the malarial vector *Anopheles stephensi* Liston (Diptera: *Culicidae*). Exp Parasitol. 2015; 153:8-16. https://doi.org/10.1016/j.exppara.2015.01.017
24. Abdelgadir AA, Ahmed EM, Eltohami MS. Isolation, characterization and quantity determination of aristolochic acids, toxic compounds in *Aristolochia bracteolata* L. Environ Health Insights. 2011; 5:1-8. PMCID: PMC3072213. PMID: 21487531. https://doi.org/10.4137/EHI.S6292
25. Zhu K, Borrelli KW, Greenwood JR, Day T, Abel R, Farid RS, *et al*. Docking covalent inhibitors: A parameter free approach to pose prediction and scoring. J Chem Inf Model. 2014; 54(7):1932-1940. https://doi.org/10.1021/ci500118s